Differential responses to CO_2 and sympathetic stimulation in the cerebral and femoral circulations in humans

Philip N. Ainslie[1], Jon C. Ashmead[1], Kojiro Ide[1], Barbara J. Morgan[2] and Marc J. Poulin[1]

[1] *Departments of Physiology & Biophysics and Clinical Neurosciences, Faculty of Medicine and Faculty of Kinesiology, University of Calgary, 3330 Hospital Drive NW, Calgary Alberta, T2N 4 N1 Canada*

[2] *Department of Orthopaedics and Rehabilitation, University of Wisconsin, Madison, WI 53706, USA*

The relative importance of CO_2 and sympathetic stimulation in the regulation of cerebral and peripheral vasculatures has not been previously studied in humans. We investigated the effect of sympathetic activation, produced by isometric handgrip (HG) exercise, on cerebral and femoral vasculatures during periods of isocapnia and hypercapnia. In 14 healthy males (28.1 ± 3.7 (mean ± S.D.) years), we measured flow velocity ($\bar{V}_P$; transcranial Doppler ultrasound) in the middle cerebral artery during euoxic isocapnia (ISO, +1 mmHg above rest) and two levels of euoxic hypercapnia (HC5, end-tidal P_{CO_2}, P_{ET,CO_2}, = +5 mmHg above ISO; HC10, P_{ET,CO_2} = +10 above ISO). Each P_{ET,CO_2} level was maintained for 10 min using the dynamic end-tidal forcing technique, during which increases in sympathetic activity were elicited by a 2-min HG at 30% of maximal voluntary contraction. Femoral blood flow (FBF; Doppler ultrasound), muscle sympathetic nerve activity (MSNA; microneurography) and mean arterial pressure (MAP; Portapres) were also measured. Hypercapnia increased $\bar{V}_P$ and FBF by 5.0 and 0.6% mmHg^{-1}, respectively, and MSNA by 20–220%. Isometric HG increased MSNA by 50% and MAP by 20%, with no differences between ISO, HC5 and HC10. During the ISO HG there was an increase in cerebral vascular resistance (CVR; 20 ± 11%), while $\bar{V}_P$ remained unchanged. During HC5 and HC10 HG, $\bar{V}_P$ increased (13% and 14%, respectively), but CVR was unchanged. In contrast, HG-induced sympathetic stimulation increased femoral vascular resistance (FVR) during ISO, HC5 and HC10 (17–41%), while there was a general decrease in FBF below ISO. The HG-induced increases in MSNA were associated with increases in FVR in all conditions (r = 0.76–0.87), whereas increases in MSNA were associated with increases in CVR only during ISO (r = 0.91). In summary, in the absence of hypercapnia, HG exercise caused cerebral vasoconstriction, myogenically and/or neurally, which was reflected by increases in CVR and a maintained $\bar{V}_P$. In contrast, HG increased FVR during conditions of ISO, HC5 and HC10. Therefore, the cerebral circulation is more responsive to alterations in P_{CO_2}, and less responsive to sympathetic stimulation than the femoral circulation.

(Resubmitted 23 March 2005; accepted after revision 11 May 2005; first published online 12 May 2005)

Corresponding author M. J. Poulin: Department of Physiology & Biophysics, Faculty of Medicine, University of Calgary, Heritage Medical Research Building Room 212, 3330 Hospital Drive NW, Calgary, Alberta T2N 4N1, Canada. Email: poulin@ucalgary.ca

An increase in arterial P_{CO_2} (P_{a,CO_2}) has a potent vasodilatory effect on cerebral vessels, and to a lesser extent in the heart and limb vasculatures. It is also well established that increases in P_{a,CO_2} elevate sympathetic nerve activity (SNA). However, the role of increases in SNA during hypercapnia on the cerebral and limb circulations is unclear. Although studies in experimental animals have shown that the cerebral vessels are richly innervated with sympathetic fibres, the functional role for these fibres seems to be limited to modulation of the cerebrovascular response to more powerful local chemical influences (e.g. P_{a,CO_2}; Edvinsson & Hamel, 2002).

Whether sympathetic outflow to cerebral vessels modulates cerebrovascular responses to CO_2 in humans is a matter of controversy, with some investigators demonstrating modulation (Jordan *et al.* 1998, 2000) and others showing none (LeMarbre *et al.* 2003; Przybylowski *et al.* 2003). However, several of these previous studies have used baroreflex unloading to increase sympathetic outflow, and it is possible that this intervention, which is known to increase sympathetic outflow to many other vascular beds, may not affect the cerebral circulation.

Potential regional differences in the effect of sympathetic stimulation on vascular resistance during elevations in

 DOI: 10.1113/jphysiol.2005.087320

end-tidal (i.e. arterial) P_{CO_2} (P_{ET,CO_2}) have not been previously studied in humans. In order to investigate such differences, we used isometric handgrip exercise to induce sympathetic activation. Because hypercapnia attenuates the cerebral vasoconstriction elicited by increases in arterial pressure (i.e. autoregulation; (Brian, 1998), we hypothesized that handgrip-induced cerebral vasoconstriction, if it occurred, would also be attenuated during elevations in P_{a,CO_2}. Because femoral vessels are not highly responsive to CO_2, and because fatiguing handgrip exercise increases muscle sympathetic nerve activity (MSNA) and vascular resistance in the resting leg (Saito *et al.* 1988; Seals, 1989), we further hypothesized that handgrip-induced femoral vasoconstriction would be preserved during hypercapnia.

Methods

Subjects

Fourteen healthy male subjects (28.1 ± 3.7 (mean ± S.D.) years) participated in this study. All subjects received verbal and written instructions outlining the experimental procedure; written informed consent was obtained, studies conformed to the standards set by the Declaration of Helsinki, and the research study was approved by the Conjoint Health Research Ethics Board at the University of Calgary (Grant ID 17156). Participants were not taking any medication, all were non-smokers, and none had any history of cardiovascular, cerebrovascular, or respiratory disease.

Protocol

The experiments were conducted in our laboratory located at 1103 m above sea level (barometric pressure 659 ± 9 mmHg). Each subject was studied on two occasions. Subjects were requested not to eat or drink caffeine-containing beverages within 4 h before their scheduled testing sessions in the laboratory. During the initial visit, resting end-tidal gases and estimates of hypoxic and hypercapnic ventilatory responses were measured, and the subjects became familiarized with the apparatus and experimental testing procedures. The individual hypoxic and hypercapnic ventilatory sensitivities were used to calculate the estimated inspired gas concentrations that were required to maintain the desired end-tidal partial pressures during the hypercapnic challenge (described below). For the next visit, subjects reported to the laboratory and conducted two repetitions of the same protocol. Each protocol was separated by a 45 min rest period.

The subject's normal P_{ET,CO_2} and P_{ET,O_2} were measured prior to the experiment, while the subject was sitting quietly and comfortably for approximately 10 min. The respired gas was sampled continuously (20 ml min^{-1}) via a fine catheter at the opening of one nostril by an adapted nasal O_2 therapy kit, and analysed for P_{O_2} and P_{CO_2} by mass spectrometer (AMIS 2000, Innovision, Odense, Denmark). Values for P_{O_2} and P_{CO_2} were sampled by a computer every 10 ms. P_{ET,O_2} and P_{ET,CO_2} were identified and recorded for each breath using a computer and dedicated software (Chamber v1.00, University Laboratory of Physiology, Oxford, UK).

Isocapnic–hypercapnic protocol

The subject breathed normally through a mouthpiece with the nose occluded by a nose clip. Respiratory volumes were measured with a turbine device and volume transducer (VMM-400, Interface Associates, CA, USA). Respiratory flow direction and timing information were obtained with a pneumotachograph and differential pressure transducer (RSS100-HR, Hans Rudolf Inc., Kansas City, MO, USA). Accurate control of the end-tidal gases was achieved using the technique of dynamic end-tidal forcing and dedicated software (BreatheM v2.07, University Laboratory of Physiology, Oxford, UK). This technique of dynamic end-tidal forcing has been described in detail elsewhere (Robbins *et al.* 1982*a*,*b*; Ainslie & Poulin, 2004).

After an 8-min lead-in period of isocapnic euoxia (P_{ET,CO_2} held at 1.0 mmHg above predetermined resting value; $P_{ET,O_2} = 88$ mmHg), subjects were instructed to perform a 2-min isometric handgrip at 30% of their predetermined maximal voluntary contraction. Subjects were instructed not to move or tense muscles other than those involved with the hand contractions, and each subject performed the handgrip exercise with their right arm. During each of the handgrip periods, subjects received visual feedback, via an oscilloscope, and verbal feedback from the experimenter to help them maintain the contraction at the desired level. A further 4 min of isocapnic euoxia followed the 2-min handgrip period. Over the next 20 min, two increases in P_{ET,CO_2} of +5.0 and +10.0 mmHg relative to isocapnia were maintained. Each P_{ET,CO_2} level was maintained for 10 min. During each P_{ET,CO_2} level, from minutes 4–6, subjects completed another 2-min isometric handgrip. Following the hypercapnic periods, one final 10-min period of isocapnic euoxia was administered with a handgrip during minutes 4–6. The experimental protocol is illustrated in Fig. 1.

Measurement of middle cerebral blood flow velocity and Doppler power signal

Backscattered Doppler signals from the middle cerebral artery (MCA) were measured continuously during the protocol using a 2 MHz pulsed Doppler ultrasound system (TC22, SciMed, Bristol, England), as previously described (Poulin & Robbins, 1996). In this study, the peak blood velocity (V_P) of the Doppler waveform, the velocity

associated with the intensity-weighted mean frequency of the Doppler spectrum (V_{IWM}), and the total power of the Doppler spectrum (P) were acquired every 10 ms and averaged over each heart beat ($\bar{V}_P$, $\bar{V}_{IWM}$, and $\bar{P}$, respectively, as previously defined (Poulin *et al.* 1998). The $\bar{V}_P$ was used as the primary index of cerebral blood flow (Poulin & Robbins, 1996). In all subjects, we measured ipsilateral MCA flow (i.e. right MCA) to minimize the effects of neuronal activation on cerebral blood flow.

Estimations of cerebrovascular resistance

Previous studies using transcranial Doppler ultrasound (TCD) to assess changes in cerebral blood velocity in response to hypercapnia or exercise have typically measured the $\bar{V}_P$ or the $\bar{V}_{IWM}$ velocity of the Doppler signal. These indices are proportional to flow only if the cross-sectional area of the vessel remains constant (Poulin & Robbins, 1996). An alternative index of cerebral blood flow is $\bar{V}_{IWM}$ multiplied by the overall power of the signal ($\bar{P}$). Because the total power of the signal is proportional to the cross-sectional area, the proposed index ($\overline{P \cdot V}_{IWM}$) allows for any changes that may occur in the cross-sectional area of the MCA (Poulin & Robbins, 1996). Therefore, to account for any cross-sectional area changes of the MCA, we used two methods to estimate cerebrovascular resistance (CVR).

$$CVR_1 = \text{Mean arterial blood pressure}/\bar{V}_P \quad (1)$$

$$CVR_2 = \text{Mean arterial blood pressure}/(\overline{P \cdot V}_{IWM}) \quad (2)$$

Measurement of heart rate and blood pressure

Mean arterial blood pressure (MAP) and heart rate (HR) were measured continuously using finger photoplethysmography (Portapress, TPD Biomedical Instrumentation, the Netherlands) and a three-lead ECG arrangement (Micromon 7142B monitor, Kontron Medical, France), respectively. The blood pressure and ECG signals, along with the transcranial Doppler waveforms, were updated every 10 ms by using a specialized data-acquisition package (BreatheM v 2.07, University Laboratory of Physiology, Oxford, UK).

Measurement of femoral blood flow

An ultrasound Doppler system (Sonos 1000, Hewlett-Packard, Andover, Massachusetts, USA) equipped with a linear phased array transducer probe, operating at an imaging frequency of 7.5 MHz and variable Doppler frequencies of 4.0–6.0 MHz, was used to measure two-dimensional (2D) femoral artery diameter and blood flow velocity at rest and during the intervention period. All measurements were performed below the inguinal ligament on the superficial femoral artery, approximately 3–5 cm distal to the bifurcation of the common femoral artery of the left leg. This position was chosen to prevent displacement of the probe during periods of heightened ventilation. Diameter measurements of the superficial femoral artery were obtained during the first 20 s of each minute under fixed perpendicular insonation at 7.5 MHz. Blood velocity measurements were obtained at a frequency of 4.0–6.0 MHz during the last 40 s of each minute, and were performed with the probe in the lowest insonation angle possible (45–60 deg). The sample volume was positioned in the centre of the artery and the ultrasound gate was adjusted to encompass the entire width of the vessel. Vessel diameter and blood

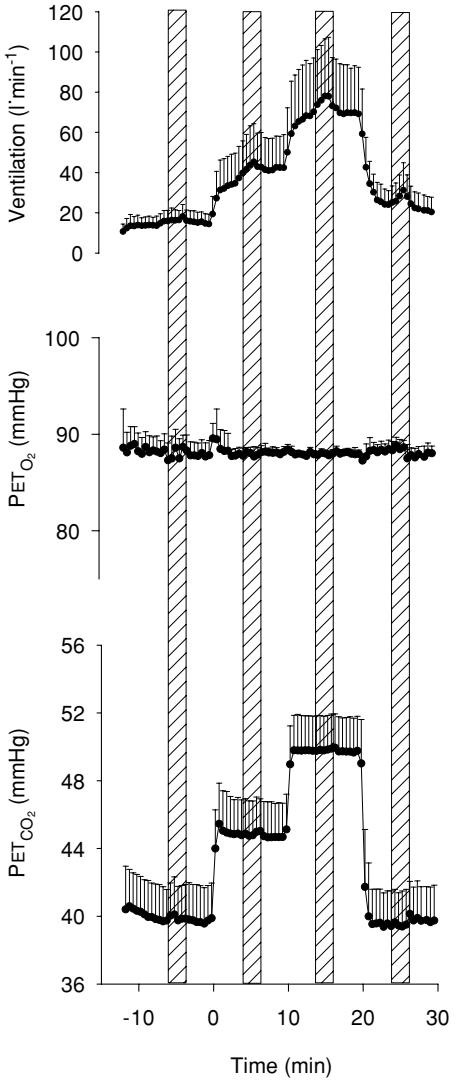

Figure 1. Schematic of the experimental protocol illustrating the time-related alterations of end-tidal P_{CO_2} (P_{ET,CO_2}), end-tidal P_{O_2} (P_{ET,O_2}), ventilatory responses and periods of handgrip (shaded columns)

Data represents 15 s averages (mean ± S.D.; $n = 14$).

velocity measurements were recorded onto a videocassette by means of an internal VCR (Panasonic, Matsushita Electrical Industrial Co., Japan), which was later used for off-line analysis.

Off-line analysis of femoral measurements. Superficial femoral artery diameter was determined from three longitudinal 2D frames, taken at end-diastole, during the initial 20 s of each minute. For each frame, three independent diameter measurements were made at different points along the vessel segment (Corretti *et al.* 2002). These diameter measurements were averaged and used to calculate the circular cross-sectional area (CSA) of the artery ($A = \pi r^2$). The envelope trace of 9–12 consecutive waveforms, during the last 40 s of each minute, was used to determine the average velocity time integral (VTI). This value multiplied by the corresponding HR and CSA, gives femoral blood flow (FBF) through the following equation:

$$\mathrm{FBF} = \mathrm{VTI} \times \mathrm{CSA} \times \mathrm{HR} \quad (3)$$

where FBF is measured in ml min^{-1}; VTI in cm beat^{-1}; CSA in cm^2 and HR in beats min^{-1}. Femoral vascular resistance (FVR) was calculated from:

$$\mathrm{FVR} = \mathrm{MAP}/\mathrm{FBF} \quad (4)$$

Muscle sympathetic nerve activity recordings

Multi-unit, postganglionic sympathetic efferent nerve activity recordings were obtained in seven subjects from the peroneal nerve using the technique of Vallbo *et al.* (1979). Placement of the recording electrode within a muscle nerve fascicle was confirmed by (1) weak electrical stimulation through the electrode elicited involuntary muscle contraction but not paresthesias; (2) tapping or stretching the muscles or tendons supplied by the impaled fascicle elicited afferent discharge, whereas stroking the skin did not; and (3) the pulse-synchronous nature of the nerve activity. MSNA recording with signal-to-noise ratios of at least 3 : 1 were considered acceptable. Neural recordings that showed evidence of alpha-motoneurone activity or mechanoreceptor activity were excluded from the analysis.

Neurogram analysis. The sympathetic neurogram was integrated off-line with the electrocardiogram (ECG), blood pressure, and respiratory signals on a time series by an interactive computer program. Sympathetic bursts were identified by computer-assisted inspection of the mean voltage neurogram. For purposes of quantification, MSNA was expressed as burst frequency (bursts min^{-1}), burst amplitude (arbitrary units), and total minute activity (burst frequency × mean burst amplitude). During the experimental protocol, MSNA was expressed as a percentage of the initial isocapnic baseline level.

Data and statistical analysis

The beat-by-beat values for $\bar{V}_P$, MAP and HR, and the breath-by-breath values for ventilation and end-tidal gases, were initially averaged over 30-s intervals over each level of P_{ET,CO_2}. Femoral blood flow, from each subject, was averaged over 60-s intervals. To calculate the percentage change from baseline, all data were averaged over the 5-min period of euoxic isocapnia immediately preceding any changes in P_{ET,CO_2} or handgrip exercise. The percentage changes in CVR_1 and FVR (Fig. 3) are expressed as changes from the initial 5 min euoxic isocapnic baseline. Data were initially tested for normality of distribution using the Shapiro–Wilk test, before being analysed by repeated-measures analysis of variance, where appropriate. *Post hoc* tests (Tukey) were performed to isolate any significant differences. Following a simple main effect and interaction, Bonferroni-corrected paired-sample *t* tests were employed to make *a posteriori* comparisons at each handgrip period and P_{ET,CO_2} level of the between-subjects factor. Non-parametric equivalents included Wilcoxon matched pairs signed ranks and Kruskal–Wallis tests. Because there were no discernible differences between the two repetitions completed by each subject, data from the two protocols were combined to optimize the signal to noise ratio and for statistical analysis. The relationship between selected dependent variables was assessed using a Pearson product moment correlation (Fig. 4). Significance for all two-tailed tests was established at an alpha level of $P < 0.05$, and data are expressed as means ± 1 standard deviation (S.D.).

Results

General observations

All 14 subjects completed the two trials, providing full data sets for the cardiorespiratory and cerebrovascular responses. MSNA data were successfully obtained from seven subjects in both tests. The unsuccessful MSNA recordings were due to alterations in nerve recording sites, loss of nerve signal, or failure to find an adequate MSNA signal. Successful FBF data were obtained in 11 subjects from both tests. The cardiorespiratory, cerebrovascular and MSNA data were not statistically different between the two trials. Therefore, data from the two tests were combined together. As illustrated in Fig. 1, the P_{ET,CO_2} and P_{ET,O_2} levels were well controlled at the desired levels throughout the experimental protocol. The general effect of both hypercapnia and handgrip-induced sympathetic activation on selected cardiorespiratory and cerebrovascular responses is outlined in Fig. 2.

Cardiorespiratory responses: effect of static handgrip exercise

During the periods of handgrip-induced sympathetic activation, there were significant increases in MSNA, MAP, heart rate, and minute ventilation during the isocapnic and hypercapnic conditions ($P < 0.05$; Table 1; Fig. 2). On average, isometric handgrip increased muscle sympathetic nerve activity by ~30–50% ($P < 0.01$), with no differences between conditions of isocapnia and hypercapnia. Mean arterial blood pressure increased significantly ($P < 0.05$) during all the periods of handgrip, with no differences between the isocapnic (ISO_1) and the hypercapnic (HC) conditions ($ISO_1 = 17.1 \pm 9.7$ mmHg; HC5, P_{ET,CO_2} $+5.0 = 19.5 \pm 8.7$ mmHg; HC10, P_{ET,CO_2} $+10.0 = 18.4 \pm 10.1$ mmHg). Similar increases in MAP were observed during the final isocapnic (ISO_2) condition. Likewise, minute ventilation was increased significantly above baseline during each period of handgrip ($ISO_1 = 4.3 \pm 7.1\,l\,min^{-1}$; $HC5 = 8.7 \pm 13.1\,l\,min^{-1}$; $HC10 = 9.4 \pm 14.3\,l\,min^{-1}$). A comparable increase from baseline in minute ventilation ($7.2 \pm 8.5\,l\,min^{-1}$; $P < 0.05$) was apparent during the final handgrip in the ISO_2 condition.

Cerebrovascular and femoral vascular responses: effect of static handgrip exercise

The total power of the Doppler signal remained stable during the periods of handgrip (Table 1), indicating that the cross-sectional area of the MCA remained relatively

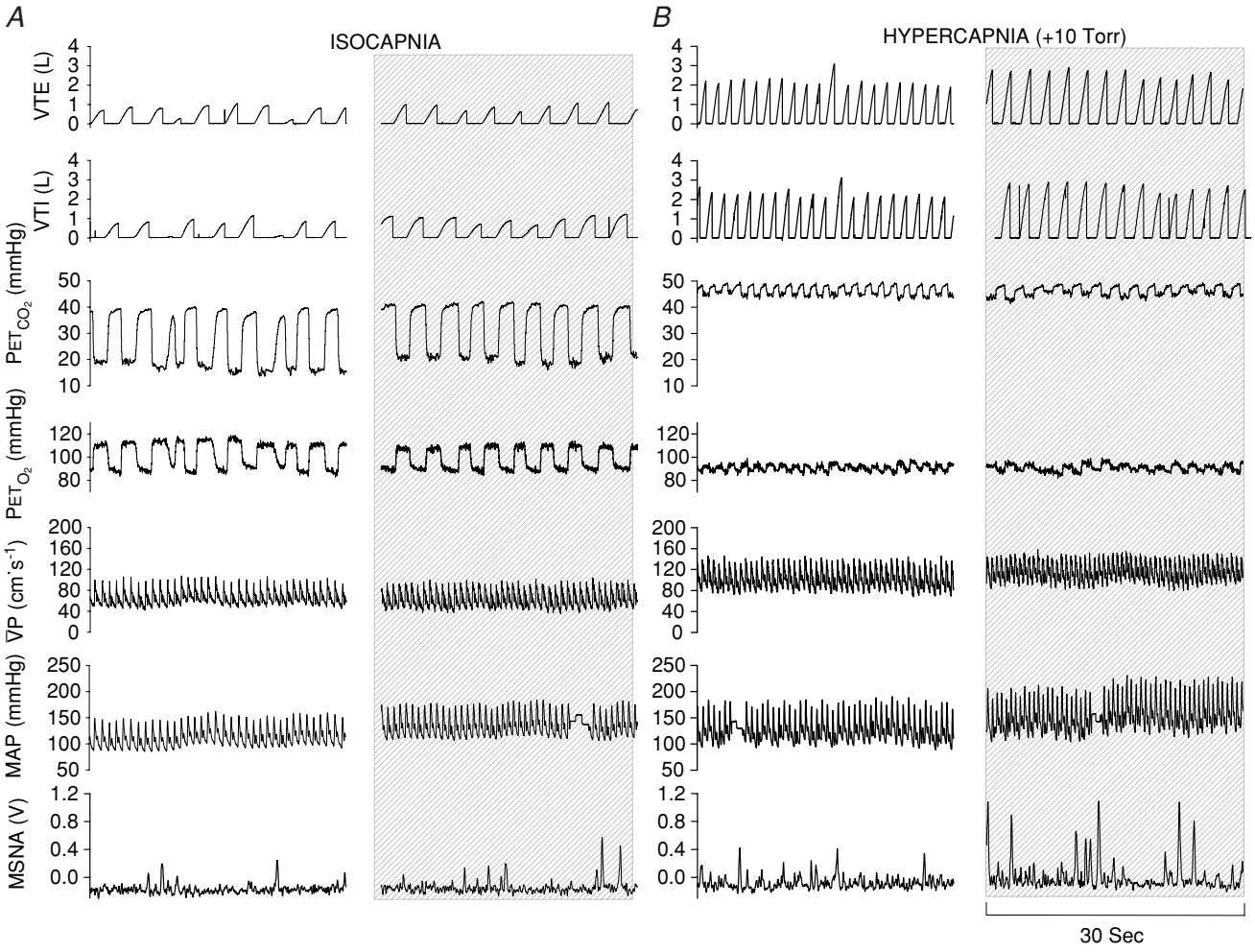

Figure 2. Representative recordings from one subject (ID, 0039) during conditions of isocapnia (*A*), 30 s before handgrip and during the last 30 s of handgrip (shaded column); and (*B*) during conditions of hypercapnia (P_{ET,CO_2} 10 mmHg above resting baseline value), 30 s before handgrip and during the last 30 s of handgrip (shaded column)

Note that during the isocapnic conditions, $\bar{V}_P$ is maintained despite elevations in MAP, indicating strong cerebral autoregulation. Conversely, during the hypercapnic conditions, increases in MAP are reflected in parallel increases in $\bar{V}_P$, suggesting a loss of cerebral autoregulation.

Table 1. Selected responses during isocapnia, hypercapnia and periods of sympathetic nerve activation

Condition	$\bar{V}_P$ (cm s^{-1})	Power (V)	CVR_1 (mmHg (cm s^{-1})$^{-1}$)	CVR_2 (mmHg %$^{-1}$)	HR (beats min^{-1})	MAP (mmHg)	MSNA[a] (%)	FBF[b] (ml min^{-1})	FVR[c] (mmHg (ml min^{-1})$^{-1}$)
ISO_1	60.2 ± 8.9	2.8 ± 0.4	1.49 ± 0.23	0.90 ± 0.14	60.4 ± 11.7	89.7 ± 9.8	100	534.4 ± 227.7	0.17 ± 0.09
ISO_1 HG	63.6 ± 11.2	2.6 ± 0.7	1.80 ± 0.32*	1.52 ± 1.9*	64.4 ± 19.2*	114.7 ± 13.8*	147.2 ± 41.9*	478.0 ± 229.1*	0.24 ± 0.11*
HC5	72.7 ± 11.3*	2.7 ± 0.4	1.28 ± 0.20	0.82 ± 0.15	65.0 ± 13.2*	93.3 ± 11.0	120.3 ± 32.1*	526.4 ± 233.3	0.18 ± 0.08
HC5 HG	81.9 ± 11.6*†	2.6 ± 0.4	1.37 ± 0.32	1.10 ± 0.30	72.8 ± 14.4*†	111.9 ± 16.3*†	176.4 ± 40.2*†	506.9 ± 219.1	0.22 ± 0.10†
HC10	87.8 ± 15.0*	2.6 ± 0.4	1.13 ± 0.24*	0.79 ± 0.16*	74.4 ± 15.6*	99.6 ± 12.1*	165.0 ± 83.0*	567.4 ± 263.5	0.18 ± 0.09
HC10 HG	100.4 ± 13.9*‡	2.5 ± 0.6	1.20 ± 0.20*	0.99 ± 0.41	84.7 ± 15.8*‡	120.3 ± 14.7*‡	189.8 ± 111.9*‡	568.0 ± 242.0	0.21 ± 0.10[b]
ISO_2	57.2 ± 10.5	2.7 ± 0.5	1.61 ± 0.33*	1.15 ± 0.41*	66.0 ± 14.1*	92.3 ± 19.7	117.8 ± 49.3	564.3 ± 277.8	0.16 ± 0.09
ISO_2 HG	65.4 ± 11.3	2.5 ± 0.7	1.90 ± 0.31*§	1.68 ± 1.56*§	76.5 ± 16.8 *[c]	124.0 ± 19.5*§	167.0 ± 81.3§	532.4 ± 260.4	0.23 ± 0.12[c]

*Significantly different from isocapnic baseline ($P < 0.05$); †significantly different from hypercapnia +5 mmHg ($P < 0.05$); ‡significantly different from hypercapnia +10 mmHg ($P < 0.05$); §significantly different from final isocapnic level ($P < 0.05$). $CVR_1 = MAP/\bar{V}_P$, $CVR_2 = MAP/(\overline{P \cdot V}_{IWM})$. [a]MSNA, data expressed as percentage change from initial isocapnic baseline; [b]femoral blood flow; [c]femoral vascular resistance, MAP/femoral blood flow.

unchanged. Application of handgrip-induced sympathetic activation produced an increase in both indices of CVR ($(MAP/\bar{V}_P)$; $(MAP/(\overline{P \cdot V}_{IWM}))$ during both the ISO_1 and ISO_2 conditions ($P < 0.05$; Table 1). Consistency between $\bar{V}_P$ and $\overline{P \cdot V}_{IWM}$ suggest that $\bar{V}_P$ is an appropriate estimation of cerebral blood flow under the experimental conditions of the present study. During the isocapnic HG there was a 20% increase in calculated CVR_1 (Table 1), while $\bar{V}_P$ remained unchanged. Conversely, during the hypercapnic conditions, $\bar{V}_P$ increased significantly by 13% and 14% during HC5 and HC10, respectively (Table 1), whereas CVR_1 remained unchanged. There were no significant differences in CVR_1 during HG-induced sympathetic activation at either HC5 or HC10. In contrast, HG-induced sympathetic stimulation produced comparable increases in FVR during the final minute of HG during each of the ISO and HC conditions (17–41%; Table 1; Fig. 3). During HG in ISO_1, there was a decrease in FBF below baseline ($P < 0.05$). Likewise, during HG in HC5 and ISO_2 there was a similar trend for a decrease in FBF ($P = 0.09$ and 0.07, respectively), whereas FBF was maintained during HG in HC10.

Cerebrovascular, cardiorespiratory and femoral responses to hypercapnia

On average, hypercapnia produced increases in minute ventilation and $\bar{V}_P$ of approximately 5.7 l min^{-1} mmHg^{-1} and 2.7 cm s^{-1} mmHg^{-1}, respectively. In ISO_2, the baseline minute ventilation remained significantly elevated when compared with ISO_1 (12.2 ± 5.6 *versus* 23.9 ± 7.0 l min^{-1}; $P < 0.01$). There were no significant differences in $\bar{V}_P$ between the ISO_1 and ISO_2 conditions. Compared to ISO_1, there were significant decreases in CVR during the HC10 level ($P < 0.05$; Table 1). Conversely, during the ISO_2 test, the baseline CVR was elevated when compared to ISO_1 ($P < 0.05$; Table 1; Fig. 2). The hypercapnic stimulus produced significant increases in heart rate, MAP and MSNA, when compared to ISO_1 (Table 1). During ISO_2, while heart rate remained elevated, there were no differences in MAP or MSNA, when compared to ISO_1.

Hypercapnia did not produce any significant changes in FBF. However, during HC10, there was a trend for an increase in FBF (534 ± 228 ml min^{-1} *versus* 568 ± 242 ml min^{-1}; $P = 0.07$; Table 1) when compared with ISO_1. As illustrated in Fig. 3, the conditions of hypercapnia produced unremarkable changes in FVR.

Relationships between changes in cerebral vascular resistance, femoral vascular resistance and muscle sympathetic nerve activity

Moderately strong, significant correlations were evident between the handgrip-induced increases in MSNA and CVR during ISO_1 ($r = 0.91$; $P < 0.01$) and ISO_2 ($r = 0.78$; $P < 0.05$). However, such relationships were not evident during HC5 ($r = –0.43$, *NS*) or HC10 ($r = 0.32$, not significant) above resting (Fig. 4). In contrast, moderately strong, significant correlations were evident between MSNA and FVR in all isocapnic and hypercapnic conditions (ISO_1, $r = 0.76$; $P < 0.05$: HC5, $r = 0.87$; $P < 0.05$: HC10.0, $r = 0.80$; < 0.05: ISO_2, $r = 0.67$; $P < 0.05$). These relationships are illustrated in Fig. 4.

Discussion

Major findings

Under isocapnic conditions, static handgrip exercise elicited an increase in CVR with unchanged $\bar{V}_P$. However, under hypercapnic conditions CVR did not increase, and $\bar{V}_P$ rose, tracking the handgrip-induced rises in arterial pressure. In contrast to the cerebral circulation, HG exercise produced significant increases in FVR in each of the isocapnic and hypercapnic conditions. Hypercapnia alone (before initiation of the HG exercise) produced small changes in FBF (0.6% mmHg^{-1}) that were unremarkable compared to those in the cerebral circulation (5.0% mmHg^{-1}). Collectively, our findings

indicate that the cerebral circulation is more responsive to alterations in P_{CO_2}, and less responsive to sympathetic stimulation than the femoral circulation. The following discussion considers the evidence, methodological assumptions and the relevance underlying the findings of this study.

Influence of autonomic nerves on cerebral blood flow

The large cerebral arteries are innervated by adrenergic fibres originating from the ipsilateral superior cervical ganglion (Itakura *et al.* 1977). Smaller arteries or arterioles have much less adrenergic innervation, and are innervated mainly by secondary systems arising from the locus ceruleus (Nielsen, 1967; Itakura *et al.* 1977). Because of differences in distribution of α and β receptors, β receptor-mediated vasodilatation occurs mainly in small cerebral vessels, while α receptor-mediated vasoconstriction preferentially affects large cerebral arteries (Fitch *et al.* 1975). Thus, at least in experimental animals, sympathetic stimulation causes vasoconstriction in large vessels. However, as long as arterial pressure remains in the autoregulatory range, there is little change in cerebral blood flow because of a concomitant decrease in pial vessel

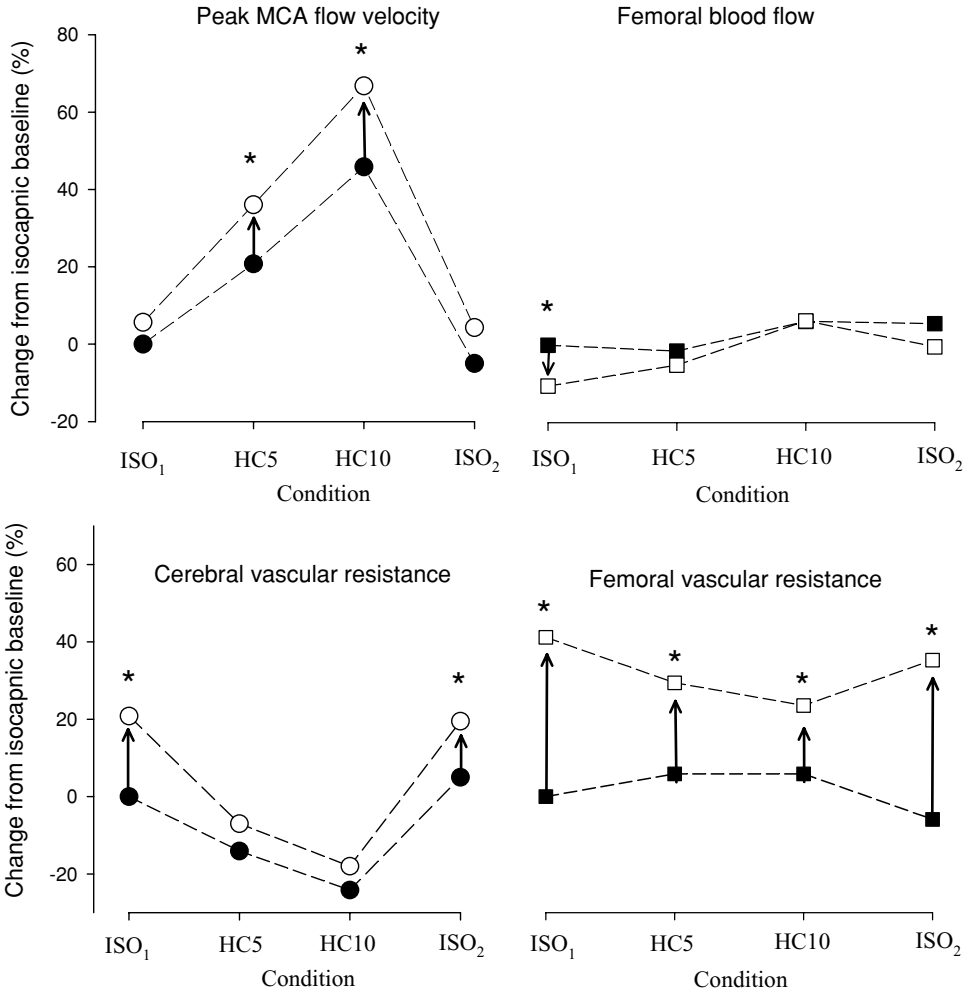

Figure 3. Percentage changes in middle cerebral artery peak blood flow velocity, femoral blood flow and cerebral and femoral vascular resistance during the isocapnic (ISO_1 and ISO_2) and hypercapnic (HC5, P_{ET,CO_2} 5 mmHg above ISO_1; HC10, P_{ET,CO_2} 10 mmHg above ISO_1) protocols
Periods of handgrip are shown by the open circles and squares. *Significant within-condition difference ($P < 0.05$) between rest and handgrip. Cerebrovascular resistance = MAP/$\bar{V}_P$ ($n = 14$) and femoral vascular resistance = MAP/FBF ($n = 11$). Data show the marked effect of hypercapnia alone in producing vasodilatation in the cerebral circulation (indicated by the decrease in CVR and increase in $\bar{V}_P$, ●), whereas there is little change in FVR and FBF in the limb with hypercapnia (■). In the femoral circulation, handgrip-induced muscle sympathetic nerve activity elicited a marked increase in FVR during isocapnic and hypercapnic conditions (□); in the cerebral circulation, the change in CVR is only evident in the isocapnic conditions (○). Arrows (→) denote significant impact of handgrip.

resistance (Baumbach & Heistad, 1983), caused by either autoregulatory or β-adrenergic vasodilatation (Sohn, 1998). In the present study, the maintainance of $\bar{V}_P$ in the presence of handgrip-induced sympathetic stimulation and arterial pressure increase during isocapnia is broadly comparable to previous results in the highly controlled rabbit and cat models (Baumbach & Heistad, 1983).

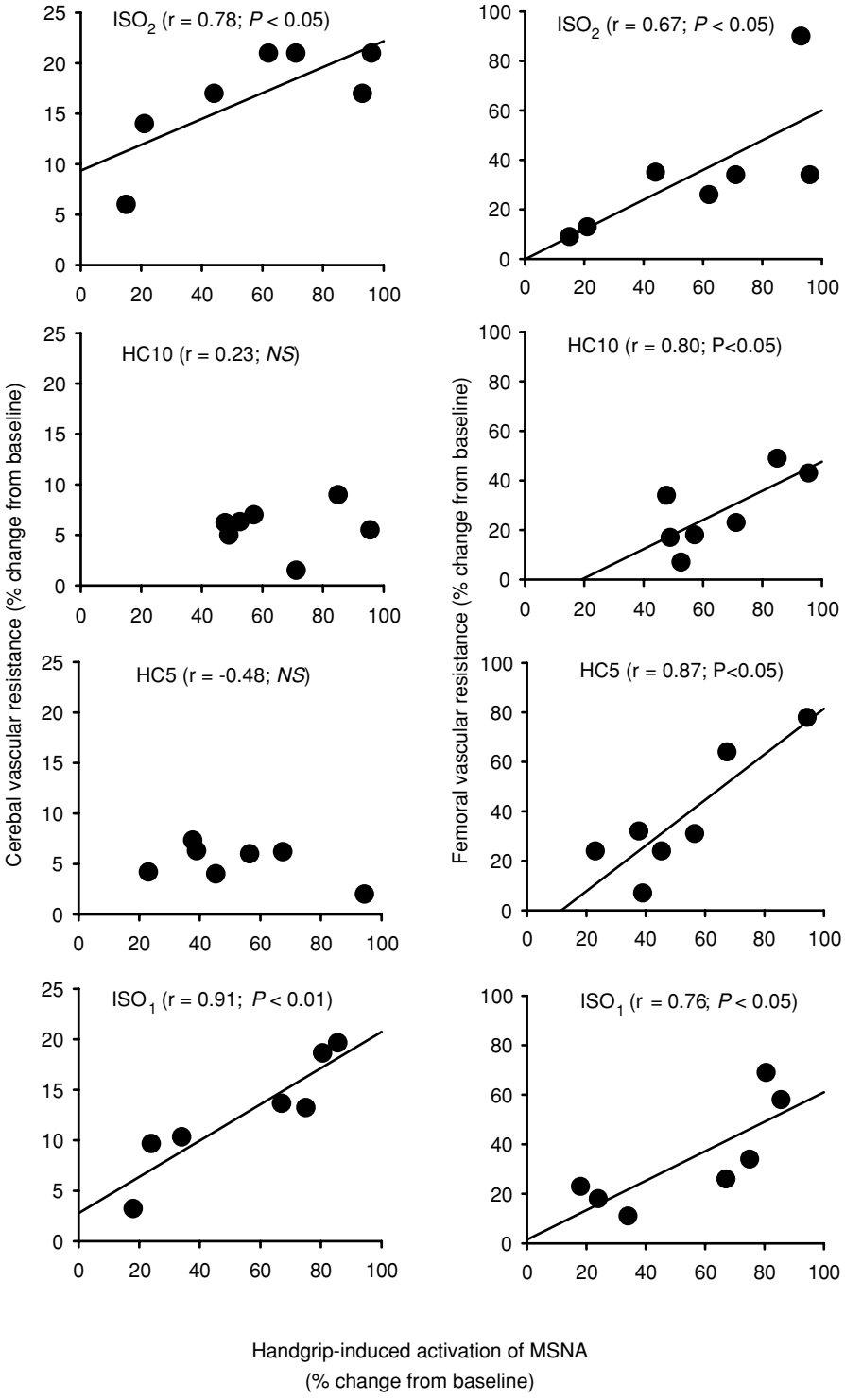

Figure 4. Relationship between handgrip-induced increases in muscle sympathetic nerve activity (MSNA) and cerebral vascular resistance (CVR, left panel) and femoral vascular resistance (FVR, right panel) during isocapnic and hypercapnic conditions
Note the strong relationships between MSNA and CVR are lost during periods of hypercapnia.

Cerebral vasoconstriction versus myogenic response

During HG performed under isocapnic conditions, we observed an increase in CVR along with unchanged $\bar{V}_P$. However, from the present experiments, we cannot be certain whether this cerebral vasoconstriction was caused by sympathetic activation *per se*, or was a myogenic response elicited by the HG-induced rise in arterial pressure. Regardless of the mechanism, such increases in CVR served to maintain a constant cerebral blood velocity in the face of a large pressure response during isocapnic handgrip. In contrast, under hypercapnic conditions, $\bar{V}_P$ tracked the handgrip-induced rise in arterial pressure, indicating a failure of neural and/or autoregulatory mechanisms. While we acknowledge that correlations cannot establish causal relationships, we did observe strong correlations between increases in MSNA and CVR during isocapnic conditions (Fig. 4), which provide some support for the notion of sympathetically mediated vasoconstriction. The mechanism(s) underlying this finding requires further investigation.

Handgrip-induced femoral vasoconstriction

Our findings, which are consistent with previous reports that leg vascular resistance and MSNA are highly correlated during fatiguing exercise (Saito *et al.* 1988; Seals, 1989), support the concept that sympathetic engagement is a major, direct vasoconstrictor mechanism in the lower limb. Although pressure-dependent (i.e. myogenic) mechanisms may also play a role (Shoemaker *et al.* 2000), we would not expect FBF to be reduced below the baseline level, as it was in this study, if only myogenic mechanisms were operative.

Differential responses between the cerebral and femoral vasculatures

In the present study, sympathetic engagement during conditions of hypercapnia caused vasoconstriction in the femoral, but not the cerebral vasculature. Why should blood vessels in the brain and leg respond differently when hypercapnia is superimposed on sympathetic activation? Several explanations for these differential sensitivities can be proposed. First, it has long been appreciated that the vasodilatory effect of hypercapnia is much more profound in the cerebral vessels than the leg vessels (Lennox & Gibbs, 1932). Indeed, in the present study, the CO_2 reactivity in the cerebral circulation was a ~5% increase in $\bar{V}_P$ for every 1 mmHg increase in P_{ET,CO_2}, whereas in the femoral circulation it was ~8-fold lower. Hypercapnic cerebral vasodilatation is a local effect with complex and perhaps redundant mechanisms (nitric oxide synthase, cyclooxygenase, P-450 oxygenase pathways have all been implicated (Iadecola & Zhang, 1994; Pelligrino *et al.* 1999; Niwa *et al.* 2001). It is not clear why CO_2 is a less potent vasodilator in the limb circulation. Second, the vasoconstrictor responsiveness of the cerebral and limb vessels is likely to be influenced by anatomical differences in the two vascular beds. There is a higher distribution of α-adrenoreceptors in the peripheral and dependent vascular beds than in the cerebral circulation, and the presence of the endothelial blood–brain barrier limits access of many circulating vasoconstrictors to vascular smooth muscle in the cerebral vessels (Faraci & Heistad, 1998). For example, recent studies which have examined the effects of intravenous infusion of various sympathomimetic drugs (ephedrine, dobutamine, dopexamine (Moppett *et al.* 2004)) and noradrenaline (Kimmerly *et al.* 2003), reported no effect of the drugs on cerebrovascular control in healthy humans.

Comparison with previous studies: the cerebrovascular 'escape' phenomenon

Results from experimental animals, during sustained sympathetic activation have shown that a 'vasomotor escape' phenomenon occurs, suggesting that neural control of the cerebral circulation may be more effective under dynamic than steady-state conditions (Sercombe *et al.* 1979; Baumbach & Heistad, 1983). The results from the present study, under 2 min of HG-induced sympathetic activation, are not consistent with such a 'vasomotor escape' phenomenon. However, the unphysiological frequencies (1–50 Hz) and patterns of stimulation used in animal studies (Sercombe *et al.* 1979; Baumbach & Heistad, 1983; Lacroix *et al.* 1988) make comparisons with human studies unrealistic.

Methodological considerations

Transcranial Doppler ultrasound. We used Doppler ultrasound to measure flow velocity in the middle cerebral artery. While this is not a direct measurement of cerebral blood flow, we believe that velocity is a reasonable estimate of flow in our experiments because: (1) the diameter of the middle cerebral artery has been shown to vary by less than 4% during changes in arterial pressure and changes in CO_2 tension (Giller *et al.* 1993; Serrador *et al.* 2000), and (2) velocity and flow through the middle cerebral artery are highly correlated (Kirkham *et al.* 1986). Our estimates of cerebrovascular CO_2 reactivity ($2.7\ cm\ s^{-1}\ mmHg^{-1}$ (~5% $mmHg^{-1}$) for hypercapnia) are consistent with previous reports which have utilized a range of different methodological techniques to assess cerebrovascular CO_2 reactivity (Kety & Schmidt, 1948; Rostrup *et al.* 1994; Ide *et al.* 2003). As evident in the present study, the total power of the Doppler signal remained stable during the periods of handgrip, indicating that the cross-sectional area of the MCA remained relatively unchanged. Furthermore, our contribution of a MCA flow index (i.e. $\overline{P \cdot V_{IWM}}$) does help to interpret the results, in that this index

corroborates the velocity measurements, as an index of flow, reported in this study. This is consistent with our previous work (Poulin & Robbins, 1996; Ainslie & Poulin, 2004) during periods of hypercapnia and hypoxia, which showed no change in the Doppler power signal. Finally, despite the limitations associated with transcranial Doppler ultrasound, this is the only method with sufficient temporal resolution to address the aims of this study.

Cerebrovascular resistance. Vascular resistance is estimated as the ratio of the pressure drop to flow across the vascular bed. In the case of CVR, calculation is complicated by unknown values of intracranial and venous pressures. However, since our subjects were positioned in a semisupine position, it is likely that the major determinant of cerebral perfusion pressure was MAP. Recent comparisons of different approaches to determining CVR have supported the use of the MAP : cerebral blood flow ratio (Schondorf *et al.* 2001). From the present study, however, it cannot be determined whether the cerebrovascular responses in the distribution of the MCA reflect global cerebral effects; e.g. discreet regions of the brain may respond differently to changes in sympathetic stimulation (Sercombe *et al.* 1975; Roatta *et al.* 2003). The novel approach in the present study is the use of a Doppler flow index in order to account for any changes in the cross-sectional area of the MCA.

Control of end-tidal gases. The combined techniques of dynamic end-tidal forcing, Doppler ultrasound and microneurography provided means to overcome many of the technical shortcomings apparent in previous studies. In the majority of these earlier studies, which have considered the role of sympathetic activation in the cerebral circulation of humans, it was not possible to achieve accurate control over the end-tidal gases because of limitations in the techniques used to administer the changes of P_{ET,CO_2} and P_{ET,O_2}. A number of these studies did not control for P_{ET,CO_2} levels (Grubb *et al.* 1991; Levine *et al.* 1994; Bondar *et al.* 1995; Zhang *et al.* 1998; Jordan *et al.* 1998; Sohn, 1998; Giller *et al.* 2000; Zhang *et al.* 2002), raising the possibility that the reported decrease in CBF was due, at least in large part, to the influence of hypocapnia rather than any influence from the autonomic nervous system. The studies that did attempt to control the end-tidal gases, involved manual switches between different fixed inspired gas mixtures (Jordan *et al.* 2000; Jordan *et al.* 2002). As such, several minutes are required before the desired end-tidal levels are reached. The dynamic end-tidal forcing system uses prediction and feedback correction (via the end-tidal gas values) to adjust the inspired gas composition on a breath-by-breath basis to hold the subject's P_{ET,CO_2} and P_{ET,O_2} levels constant despite changes in ventilation. It is well established that arterial P_{CO_2} is the most potent regulator of the cerebral circulation (Brian, 1998). Since we observed modest but significant increases in ventilation (4–10 l min^{-1}) during the periods of handgrip, it is clear that precise control of the P_{ET,CO_2} gas levels is critical in the interpretation and understanding of the influence of sympathetic activation on CBF regulation. Inadequate control of P_{ET,CO_2} during periods of sympathetic stimulation may well be one important factor contributing to the controversy surrounding the neural control of the cerebral circulation in humans. While this study did not include direct measurements of arterial P_{CO_2} and P_{O_2}, end-tidal values of P_{CO_2} and P_{O_2} have been shown to be appropriate estimates of arterial values in similar conditions to those of the present study, in individuals free of respiratory disease (Robbins *et al.* 1990).

Summary and relevance

During isocapnia, HG caused an increase in CVR, while $\bar{V}_P$ was unchanged; conversely, under hypercapnic conditions, CVR was unchanged and $\bar{V}_P$ was elevated. In the femoral circulation, HG exercise significantly elevated FVR in both isocapnic and hypercapnic conditions. Hypercapnia (before initiation of the HG exercise) produced unremarkable changes in FBF (0.6% mmHg^{-1}) compared to those in the cerebral circulation (5.0% mmHg^{-1}).

The fact that the circulatory adjustments of the cerebral vasculature are seemingly opposite to those of the femoral vasculature is of teleological relevance. If vessels in the cerebral and femoral vasculatures were both to dilate to the same extent in response to increased arterial P_{CO_2}, there would be a dramatic fall in systemic blood pressure. Sympathetic stimulation seems to play a major vasoconstrictor role in the femoral vasculature, but a less prominent role in the cerebral vasculature. The main functional relevance of sympathetically mediated cerebral vasoconstriction may be to protect the blood–brain barrier from overperfusion during periods of acute hypertension, when the limits of autoregulation are compromised (Mayhan *et al.* 1987). The high resting metabolic requirements of the brain, compared with that of the femoral vasculature, might be another reason why this circulatory arrangement is desirable, i.e. high CO_2 sensitivity is a way for the brain to match metabolism with flow. On the other hand, sympathetic vasoconstriction is a way to redistribute cardiac output from non-essential to essential vascular beds under conditions of environmental change (posture, exercise, heat/cold). Since there is probably no condition where the cerebral circulation would be considered non-essential, it seems desirable for the brain to have limited capacity for vasoconstriction.

References

Ainslie PN & Poulin MJ (2004). Ventilatory, cerebrovascular, and cardiovascular interactions in acute hypoxia: regulation by carbon dioxide. *J Appl Physiol* **97**, 149–159.

Baumbach GL & Heistad DD (1983). Effects of sympathetic stimulation and changes in arterial pressure on segmental resistance of cerebral vessels in rabbits and cats. *Circ Res* **52**, 527–533.

Bondar RL, Kassam MS, Stein F, Dunphy PT, Fortney S & Riedesel ML (1995). Simultaneous cerebrovascular and cardiovascular responses during presyncope. *Stroke* **26**, 1794–1800.

Brian JE (1998). Carbon dioxide and the cerebral circulation. *Anesthesiology* **88**, 1365–1386.

Corretti MC, Anderson TJ, Benjamin EJ, Celermajer D, Charbonneau F, Creager MA, Deanfield J, Drexler H, Gerhard-Herman M, Herrington D, Vallance P, Vita J & Vogel R (2002). Guidelines for the ultrasound assessment of endothelial-dependent flow-mediated vasodilation of the brachial artery: a report of the International Brachial Artery Reactivity Task Force. *J Am Coll Cardiol* **39**, 257–265.

Edvinsson L & Hamel E (2002). Perivascular nerves in brain vessels. In *Cerebral Blood Flow and Metabolism*, 2nd edn, ed. Edvinsson L & Krause DN, pp. 43–67. Lippincott. Williams & Wilkins, Philadelphia.

Faraci FM & Heistad DD (1998). Regulation of cerebral circulation: role of endothelium and potassium channels. *Physiol Rev* **78**, 53–97.

Fitch W, MacKenzie ET & Harper AM (1975). Effects of decreasing arterial blood pressure on cerebral blood flow in the baboon. Influence of the sympathetic nervous system. *Circ Res* **37**, 550–557.

Giller CA, Bowman G, Dyer H, Mootz L & Krippner W (1993). Cerebral arterial diameters during changes in blood pressure and carbon dioxide during craniotomy. *Neurosurgery* **32**, 737–742.

Giller CAGI, Iler AM, Cooper CR & Hatab MR (2000). Evaluation of the cerebral hemodynamic response to rhythmic handgrip. *J Appl Physiol* **88**, 2205–2213.

Grubb BP, Gerard G, Roush K, Temesy-Armos P, Montford P, Elliott L, Hahn H & Brewster P (1991). Cerebral vasoconstriction during head-upright tilt-induced vasovagal syncope. A paradoxic and unexpected response. *Circulation* **84**, 1157–1164.

Iadecola C & Zhang F (1994). Nitric oxide- dependent and independent components of cerebrovasodilation elicited by hypercapnia. *Am J Physiol* **266**, R546–R552.

Ide K, Eliasziw M & Poulin MJ (2003). The relationship between middle cerebral artery blood velocity and end-tidal P_{CO_2} in the hypocapnic-hypercapnic range in humans. *J Appl Physiol* **95**, 129–137.

Itakura T, Yamamoto K, Tohyama M & Shimizu N (1977). Central dual innervation of arterioles and capillaries in the brain. *Stroke* **8**, 360–365.

Jordan J, Shannon JR, Black BK, Paranjape SY, Barwise J & Robertson D (1998). Raised cerebrovascular resistance in idiopathic orthostatic intolerance – Evidence for sympathetic vasoconstriction. *Hypertension* **32**, 699–704.

Jordan J, Shannon JR, Diedrich A, Black B, Costa F, Robertson D & Biaggioni I (2000). Interaction of carbon dioxide and sympathetic nervous system activity in the regulation of cerebral perfusion in humans. *Hypertension* **36**, 383–388.

Jordan J, Shannon JR, Diedrich A, Black BK & Robertson D (2002). Increased sympathetic activation in idiopathic orthostatic intolerance – Role of systemic adrenoreceptor sensitivity. *Hypertension* **39**, 173–178.

Kety SS & Schmidt CF (1948). The effects of altered arterial tensions of carbon dioxide and oxygen on cerebral blood flow and cerebral oxygen consumption of normal young men. *J Clin Invest* **27**, 484–492.

Kimmerly DS, Tutungi E, Wilson TD, Serrador JM, Gelb AW, Hughson RL & Shoemaker JK (2003). Circulating norepinephrine and cerebrovascular control in conscious humans. *Clin Physiol Funct Imaging* **23**, 314–319.

Kirkham FJ, Padayachee TS, Parsons S, Seargeant LS, House FR & Gosling RG (1986). Transcranial measurement of blood velocities in the basal cerebral arteries using pulsed Doppler ultrasound: velocity as an index of flow. *Ultrasound Med Biol* **12**, 15–21.

Lacroix JS, Stjarne P, Anggard A & Lundberg JM (1988). Sympathetic vascular control of the pig nasal mucosa (1): Increased resistance and capacitance vessel responses upon stimulation with irregular bursts compared to continuous impulses. *Acta Physiol Scand* **132**, 83–90.

LeMarbre G, Stauber S, Khayat RN, Puleo DS, Skatrud JB & Morgan BJ (2003). Baroreflex-induced sympathetic activation does not alter cerebrovascular CO_2 responsiveness in humans. *J Physiol* **551**, 609–616.

Lennox WG & Gibbs EL (1932). The blood flow in the brain and leg of man, and the changes induced by alteration of blood gases. *J Clin Invest* **11**, 1155–1177.

Levine BD, Giller CA, Lane LD, Buckey JC & Blomqvist CG (1994). Cerebral versus systemic hemodynamics during graded orthostatic stress in humans. *Circulation* **90**, 298–306.

Mayhan WG, Werber AH & Heistad DD (1987). Protection of cerebral vessels by sympathetic nerves and vascular hyperthrophy. *Circulation* **75**, I107–I112.

Moppett IK, Wild MJ, Sherman RW, Latter JA, Miller K & Mahajan RP (2004). Effects of ephedrine, dobutamine and dopexamine on cerebral haemodynamics: transcranial Doppler studies in healthy volunteers. *Br J Anaesth* **92**, 39–44.

Nielsen KC (1967). Adrenergic innervation of pial arteries related to the circle of Willis in the cat. *Brain Res* **6**, 770–772.

Niwa K, Haensel C, Ross ME & Iadecola C (2001). Cyclooxygenase-1 participates in selected vasodilator responses of the cerebral circulation. *Circ Res* **88**, 600–608.

Pelligrino DA, Santizo RA & Wang Q (1999). Miconazole represses CO_2-induced pial arteriolar dilation only under selected circumstances. *Am J Physiol* **277**, H1484–H1490.

Poulin MJ, Liang P-J & Robbins PA (1998). Fast and slow components of the cerebral blood flow response to step decreases in end-tidal PCO_2 in humans. *J Appl Physiol* **85**, 388–397.

Poulin MJ & Robbins PA (1996). Indexes of flow and cross-sectional area of the middle cerebral artery using Doppler ultrasound during hypoxia and hypercapnia in humans. *Stroke* **27**, 2244–2250.

Przybylowski T, Bangash MF, Reichmuth K, Morgan BJ, Skatrud JB & Dempsey JA (2003). Mechanisms of the cerebrovascular response to apnoea in humans. *J Physiol* **548**, 323–332.

Roatta S, Canova D, Bosone D, Micieli G & Passatore M (2003). Noradrenergic constriction of cerebral arteries as detected by transcranial Doppler (TCD) in the rabbit. *Ultrasound Med Biol* **29**, 1397–1404.

Robbins PA, Conway J, Cunningham DA, Khamnei S & Paterson DJ (1990). A comparison of indirect methods for continuous estimation of arterial P_{CO_2} in men. *J Appl Physiol* **68**, 1727–1731.

Robbins PA, Swanson GD & Howson MG (1982*a*). A prediction correction scheme for forcing alveolar gases along certain time courses. *J Appl Physiol* **52**, 1353–1357.

Robbins PA, Swanson GD, Micco AJ & Schubert WP (1982*b*). A fast gas-mixing system for breath-to-breath respiratory control studies. *J Appl Physiol* **52**, 1358–1362.

Rostrup E, Larsson HBW, Toft PB, Thomsen C, Ring P, Sondergaard L & Henriksen O (1994). Functional MRI of CO_2 induced increase in cerebral perfusion. *NMR Biomed* **7**, 29–34.

Saito M, Mano T, Iwase S, Koga K, Abe H & Yamazaki Y (1988). Responses in muscle sympathetic activity to acute hypoxia in humans. *J Appl Physiol* **65**, 1548–1552.

Schondorf R, Stein R, Roberts R, Benoit J & Cupples W (2001). Dynamic cerebral autoregulation is preserved in neurally mediated syncope. *J Appl Physiol* **91**, 2493–2502.

Seals DR (1989). Sympathetic neural discharge and vascular resistance during exercise in humans. *J Appl Physiol* **66**, 2472–2478.

Sercombe R, Aubineau P, Edvinsson L, Mamo H, Owman CH, Pinard E & Seylaz J (1975). Neurogenic influence on local cerebral blood flow. Effect of catecholamines or sympathetic stimulation as correlated with sympathetic innervation. *Neurology* **25**, 954–963.

Sercombe R, Lacombe P, Aubineau P, Mamo H, Pinard E, Reynier-Rebuffel AM & Seylaz J (1979). Is there an active mechanism limiting the influence of the sympathetic system on the cerebral vascular bed? Evidence for vasomotor escape from sympathetic stimulation in the rabbit. *Brain Res* **164**, 81–102.

Serrador JM, Picot PA, Rutt BK, Shoemaker JK & Bondar RL (2000). MRI measures of middle cerebral artery diameter in conscious humans during simulated orthostasis. *Stroke* **31**, 1672–1678.

Shoemaker JK, Herr MD & Sinoway LI (2000). Dissociation of muscle sympathetic nerve activity and leg vascular resistance in humans. *Am J Physiol Heart Circ Physiol* **279**, H1215–H1219.

Sohn YH (1998). Cerebral hemodynamic changes induced by sympathetic stimulation tests. *Yonsei Med J* **39**, 322–327.

Vallbo AB, Hagbarth KE, Torebjork HE & Wallin BG (1979). Somatosensory, proprioceptive, and sympathetic activity in human peripheral nerves. *Physiol Rev* **59**, 919–957.

Zhang R, Zuckerman JH, Iwasaki K, Wilson TE, Crandall CG & Levine BD (2002). Autonomic neural control of dynamic cerebral autoregulation in humans. *Circulation* **106**, 1814–1820.

Zhang R, Zuckerman JH & Levine BD (1998). Deterioration of cerebral autoregulation during orthostatic stress: insights from the frequency domain. *J Appl Physiol* **85**, 1113–1122.

Acknowledgements

This project was supported by the Alberta Heritage Foundation for Medical Research (AHFMR), Heart and Stroke Foundation of Alberta, NWT, & Nunavut and the Canadian Institutes of Health Research (CIHR). PNA is supported by a Focus-on-Stroke post-doctoral fellowship (Heart and Stroke Foundation of Canada, the Canadian Stroke Network, CIHR, and AstraZeneca Canada). MJP is a CIHR New Investigator and AHFMR Medical Scholar. We extend our gratitude to Professor PA Robbins for assistance in setting up the dynamic end-tidal forcing technique in Calgary, and to JS Vantanajal for skilled technical support.